biology

MDPI

Article

Leaf Structural, Photosynthetic, and Selected Metabolic Traits of Diploid and Triploid *Choerospondias axillaris* Germplasm

Tianhe Zhang [1,†], Fangdi Li [1,†], Weimin He [2], Xueqing Cui [1], Yizhou Li [1], Huashan Ling [3], Hequn Gu [3], Houlin He [3], Jiyan Liu [3] and Qirong Guo [1,*]

[1] Co-Innovation Center for Sustainable Forestry in Southern China, College of Forestry and Grassland, College of Soil and Water Conservation, Nanjing Forestry University, Nanjing 210037, China
[2] Seedling Research Institute, Jiangxi Environmental Engineering Vocational College, Ganzhou 341000, China
[3] Jiangxi Qiyunshan Food Co., Ltd., Ganzhou 341300, China
* Correspondence: qrguo@njfu.edu.cn
† These authors contributed equally to this work.

Simple Summary

Choerospondias axillaris is a wild fruit tree with both medicinal and edible value, but its polyploid germplasm has not been well studied. This study presents the first comparison of diploid and natural triploid *C. axillaris* accessions. We found that triploid plants generally had larger leaves with larger but fewer stomata and higher soluble protein content. However, no statistically detectable difference in net photosynthetic rate was observed between diploid and triploid plants, and differences in the measured photosynthetic parameters may be associated with genetic differences among cultivars rather than with ploidy level. These results indicate that triploid *C. axillaris* has distinct leaf structural and protein content characteristics, which may provide a reference for polyploid breeding in this species.

Abstract

Choerospondias axillaris is a wild fruit tree resource with both medicinal and edible value, yet the potential of its polyploid germplasm remains underexplored. This study presents the first comparison of four diploid and four natural triploid *C. axillaris* accessions in terms of leaf structure, photosynthetic characteristics, and three leaf metabolite classes. Leaf morphology, stomatal traits, gas exchange, chlorophyll fluorescence, and the contents of soluble sugars, soluble protein, and total flavonoids were measured. Triploid cultivars generally had larger leaves than diploids, with lower stomatal density and greater stoma length and stoma width, i.e., a "larger but fewer" stomatal configuration. Among these structural traits, stomatal density and stoma length were mainly associated with ploidy, whereas stoma width was also significantly affected by cultivar (genotype) differences. Triploid cultivars showed significantly higher soluble protein content, whereas flavonoid and soluble sugar contents showed no significant ploidy effect. The accumulation of all three metabolite classes was strongly influenced by genotypic differences among cultivars. However, the ploidy effects on net photosynthetic rate, stomatal conductance, and transpiration rate were all non-significant, and variation in these parameters may be associated mainly with genotypic differences among cultivars rather than with ploidy level. The maximum photochemical efficiency of all cultivars was within the normal range for healthy plants, with no statistically detectable ploidy effect. In summary, among the traits measured here, the advantages of triploid C. axillaris were manifested in leaf structure and soluble protein content, whereas no statistically detectable, general enhancement of net photosynthetic rate was associated with the triploid level. These results provide data support for polyploid breeding and superior germplasm selection in *C. axillaris*.

Check for updates

Academic Editor: Frank H. Hellwig

Received: 17 October 2026
Revised: 12 November 2026
Accepted: 16 November 2026
Published: 18 November 2026

Copyright: © 2026 by the authors. Licensee MDPI, Basel, Switzerland. This article is an open access article distributed under the terms and conditions of the Creative Commons Attribution (CC BY) license.

Keywords: *Choerospondias axillaris*; triploid; leaf structure; photosynthetic characteristics; selected metabolites; nested ANOVA

1. Introduction

Choerospondias axillaris is a native tree species belonging to the Anacardiaceae family, widely distributed across tropical and subtropical regions of Asia, spanning southern China, Southeast Asia, South Asia, and parts of East Asia [1]. This species has been established as a cultivated fruit tree in large-scale plantations, particularly in China. Its fruit is rich in nutrients and contains various bioactive compounds, demonstrating significant antioxidant activity [2–6]. Furthermore, different parts of the plant possess medicinal value: flavonoids from its leaves exhibit anti-arrhythmic properties [7], polyphenols from the fruit show anti-inflammatory and anti-cancer effects [3,8], and bark extracts have potential application in treating burns [9].

Polyploidy, referring to the condition where an organism possesses more than two complete sets of chromosomes in its sporophytic generation, is widespread in the plant kingdom [10,11]. For instance, natural triploid individuals have been found in *Toxicodendron vernicifluum*, which belongs to the same family, Anacardiaceae, as *C. axillaris* [12,13]. Natural polyploids of *Ginkgo biloba* have also been recorded in Europe [14]. Polyploidy is particularly common in Theaceae species; *Camellia oleifera* is a natural hexaploid [15], and *Camellia vietnamensis*, predominantly hexaploid, may include octoploid types according to recent findings [16]. Similarly, polyploidy is frequent in important economic crops, including fruit trees like apple (*Malus pumila*) and citrus (*Citrus reticulata*) [17,18], as well as field crops such as wheat (*Triticum aestivum*) [19] and cotton (*Gossypium hirsutum*) [20]. The polyploid materials of *C. axillaris* used in this study are all naturally occurring triploids.

Polyploids often exhibit phenotypes and physiological characteristics markedly different from their diploid counterparts and can broadly influence the synthesis and accumulation of plant metabolites [21,22]. Morphological and structural changes induced by polyploidy have been systematically observed in numerous species. For example, polyploid poplars *(Populus* hybrids) show significantly greater tree height and diameter at breast height compared to their diploid controls [23], along with a higher net photosynthetic rate [24]. Tetraploid pear (*Pyrus communis*) exhibits larger stomata, lower stomatal density, and increased leaf mass per area compared to diploids [25]. Similarly, tetraploid *Citrus* × *junos* also has larger leaves, larger stomata, and lower stomatal density, accompanied by significantly increased levels of metabolites related to stress response in the leaves [26]. Tetraploid *Liriodendron* × *sinoamericanum* possesses larger leaves, enhanced photosynthetic capacity, and significantly greater accumulation of sugars and starch in its leaves compared to the diploid [27]. Regarding metabolic physiology, polyploidization also exerts significant regulatory effects. Chromosome doubling in *Artemisia annua* can upregulate the expression of key enzyme genes in the artemisinin biosynthetic pathway, thereby promoting the accumulation of artemisinin [28]. The concentrations of various metabolites changed significantly in the leaves of tetraploid *Talinum paniculatum*, further illustrating the broad impact of polyploidization on plant metabolic networks [29].

Although extensive physiological and metabolic variation has been observed in polyploids of many plant species, comparative studies on leaf structure, photosynthetic characteristics, and metabolite accumulation between diploid and triploid *C. axillaris* have not been previously reported. In this study, four diploid and four natural triploid *C. axillaris* accessions were compared in terms of leaf morphology, anatomy, stomatal traits, gas ex-

change, chlorophyll fluorescence, and selected metabolites, with the aim of providing data support for polyploid breeding and superior germplasm selection in this species.

2. Materials and Methods

2.1. Plant Materials

This study utilized grafted plants of eight *C. axillaris* varieties. The diploid varieties included QY1, QY7, QY13, and QY15, while the triploid varieties included QY16, QY17, QY18, and QY19 (Figure 1). The accession codes QY1, QY7, QY13, QY15, QY16, QY17, QY18, and QY19 are used in this study; their correspondence to the original accession codes in Li et al. [4] (QYS1, QYS7, QYS13, QYS15, QYS16, QYS17-1, QYS18, and QYS19, respectively) is listed in Supplementary Table S1. All experimental materials were collected from the *C. axillaris* germplasm repository located in Chongyi County, Ganzhou City, Jiangxi Province, China (25°41′ N, 114°18′ E). The original trees of these eight accessions occur naturally in the wild and were collected from their natural habitats; scions were then grafted onto one-year-old rootstocks and maintained in the germplasm repository for uniform management. These eight accessions were selected from the 47 diploid and 11 triploid accessions reported in Li et al. [4] because their ploidy had been confirmed by flow cytometry, they had been grafted in the same year (2016) onto one-year-old rootstocks and showed similar growth vigor under uniform orchard management, and together they covered different geographical origins (Guangdong, Jiangxi, Hunan, and Guangxi provinces).

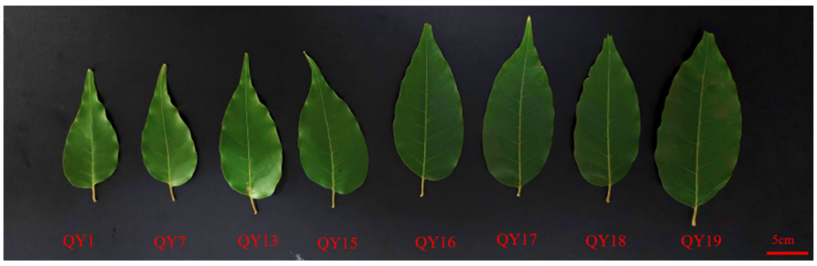


Figure 1. Appearance of the third leaflet (from the top) in compound leaves of eight *C. axillaris* cultivars.

The ploidy levels of the corresponding accessions were previously determined by flow cytometry in Li et al. [4]. In that study, rice (*Oryza sativa* subsp. *japonica* 'Nipponbare', 2C = 0.91 pg) or tomato (*Solanum lycopersicum* L. LA2683, 2C = 0.92 pg) was used as the internal standard, and ploidy was determined by comparing the relative fluorescence intensity of the G1 peaks of the sample and the internal standard. The four diploid accessions (QY1, QY7, QY13, and QY15) and four triploid accessions (QY16, QY17, QY18, and QY19) used in this study all came from the above-identified materials. The corresponding accession numbers, internal standards, ploidy levels, C values, genome sizes, and coefficients of variation are shown in Supplementary Table S1.

The germplasm sources and propagation information of the eight accessions are shown in Supplementary Table S2. All experimental plants were grafted, and the grafting year was 2016 for all accessions. The rootstocks were one-year-old seedlings. The eight accessions were planted in the same experimental orchard with a spacing of 5 m × 5 m and managed under uniform irrigation, fertilization, pruning, and pest control practices.

2.2. Leaf Morphological Trait Measurement

Healthy, fully expanded compound leaves were collected from the middle–upper canopy of ten selected trees per cultivar. From each tree, five compound leaves were selected, and the third and fourth leaflets from the top of each compound leaf were used

for measurement, giving ten leaflets per tree [30]. Leaflet length, width, and area were measured using ImageJ software (version 1.54g). After measurement, the leaflets were oven-dried at 60 °C to constant weight, which was recorded as the leaf dry weight. Leaf mass per area (LMA, g m^{-2}) was then calculated accordingly [31]. The values of the ten leaflets from each tree were averaged as one biological replicate, giving ten biological replicates per cultivar.

2.3. Scanning Electron Microscopy Observation

Leaf samples from *C. axillaris* of different ploidies were cut into 0.2 cm × 0.2 cm pieces. The sample surfaces were gently rinsed with PBS (Servicebio, G0002, Wuhan, China) and fixed in 3% glutaraldehyde at room temperature for 2 h. Subsequently, the samples were dehydrated through a graded ethanol series (30%, 50%, 70%, 80%, 90%, 95%, and 100%), subjected to critical point drying, mounted on aluminum stubs using double-sided carbon conductive tape, and sputter-coated with gold. Images were captured with an FEI Quanta 200 scanning electron microscope (FEI, Hillsboro, OR, USA). Stomatal parameters of *C. axillaris* leaves were measured using ImageJ software (version 1.54g).

For each cultivar, three independent trees were selected as biological replicates. From each tree, three to five healthy, fully expanded leaves were collected and cut into 0.2 cm × 0.2 cm segments, and three segments per tree were examined under the SEM. From these three segments of each tree, a total of five randomly selected 400× SEM fields (0.1303409 mm^2 each) of the abaxial epidermis were examined to count stomata. The stomatal density values from these five fields were averaged to represent that tree. Additionally, at least 50 randomly selected stomata were measured across these five fields for each tree, and the mean value was calculated to represent that tree.

2.4. Chlorophyll Fluorescence Parameter Measurement

Chlorophyll fluorescence parameters were measured using an FMS-2 Pulse Modulated Fluorometer (Hansatech, Pentney, UK). Prior to measurement, leaf sections (avoiding the midvein) were dark-adapted for 30 min using a leaf clip (Hans Scientific Instruments Co., Ltd., Shenzhen, China). Immediately after removing the clip, the initial fluorescence (F_0) was measured, followed by the application of a saturating pulse of light (0.8 s, intensity ≥3000 μmol m^{-2} s^{-1}) to obtain the maximum fluorescence (F_m). The variable fluorescence ($F_v = F_m - F_0$) and the maximum photochemical efficiency of PSII (F_v/F_m) were calculated [32]. For each cultivar, five trees were selected. On each tree, three technical measurements were performed at different positions on the same leaf, and the average of the three measurements was used as one biological replicate. Five biological replicates were thus obtained for each cultivar.

2.5. Photosynthetic Parameter Measurement

In August, on clear days between 9:00 and 11:00 AM, the photosynthetic characteristics of functional leaves of *C. axillaris* of different ploidies were measured using a CIRAS-3 portable photosynthesis system (PP Systems, Amesbury, MA, USA). The CO_2 concentration in the leaf chamber was maintained at 400 μmol mol^{-1}, the relative air humidity was set at 75%, and the temperature was maintained at 25 °C. Under a photosynthetically active radiation (PAR) of 1000 μmol m^{-2} s^{-1} and a CO_2 concentration of 400 μmol mol^{-1}, with temperature and humidity controlled to match ambient conditions, photosynthetic parameters—including the net photosynthetic rate P_n (μmol m^{-2} s^{-1}), stomatal conductance G_s (mmol m^{-2} s^{-1}), intercellular CO_2 concentration C_i (μmol mol^{-1}), and transpiration rate T_r (mmol m^{-2} s^{-1})—were measured and recorded using the same plants and leaf samples. Before each measurement, the target leaf was enclosed in the leaf chamber and exposed to

actinic light (1000 μmol m^{-2} s^{-1}) for 5–8 min of pre-illumination. The measurement was initiated only after stomatal conductance readings stabilized (fluctuation < 5% over 2 min). For each cultivar, five trees were selected. On each tree, three technical measurements were performed at different positions on the same leaf, and the average of the three measurements was used as one biological replicate. Five biological replicates were thus obtained for each cultivar.

Light-response curves were measured for four representative cultivars (QY1, QY15, QY16, and QY19), with two cultivars per ploidy level. Based on the results of the gas-exchange measurements, the cultivars with the highest net photosynthetic rates within each ploidy level (QY1 and QY15 for diploids, QY16 and QY19 for triploids) were selected to compare their responses under varying light intensities. For each of the four cultivars, three trees were selected. On each tree, three technical measurements were performed at different positions on the same leaf, and the average of the three measurements was used as one biological replicate. Three biological replicates were thus obtained for each cultivar. The red-blue LED light source was adjusted to a series of 14 PAR levels: 0, 50, 100, 150, 200, 300, 400, 600, 800, 1000, 1200, 1400, 1700, and 2000 μmol m^{-2} s^{-1}. P_n was measured at each PAR level, and the curves were fitted using a modified rectangular hyperbola model [33]:

$$P_n(I) = \alpha \frac{1 - \beta I}{1 - \gamma I} I - R_d$$

where $P_n(I)$ is the net photosynthetic rate (μmol m^{-2} s^{-1}); α is the initial quantum efficiency (μmol μmol^{-1}); β is a correction coefficient (μmol m^{-2} s^{-1}); γ is a fitted parameter (μmol m^{-2} s^{-1}); I is the photosynthetically active radiation (μmol m^{-2} s^{-1}); and Rd is the dark respiration rate (μmol m^{-2} s^{-1}). Each cultivar was fitted separately, and the coefficient of determination (R^2) was greater than 0.9 for all fitted curves.

2.6. Metabolite Content Determination

Fresh leaf samples of *C. axillaris* were divided into two portions for different extraction procedures. For the determination of soluble sugar and flavonoid contents, leaf samples were sealed in paper bags, de-enzymed at 105 °C for 30 min, and subsequently dried at 60 °C until constant weight was achieved. After drying, the petioles were removed and the leaves were ground into fine powder using a grinding mill, followed by sieving and storage in sealed bags for subsequent analysis. The soluble sugar content was determined using the anthrone colorimetric method [34] and expressed on a dry weight (DW) basis (mg g^{-1} DW). For total flavonoid content, the sodium nitrite–aluminum nitrate colorimetric method was employed. This method is based on the principle that, in alkaline sodium nitrite solution, flavonoids form red complexes with aluminum ions (Al^{3+}), which exhibit a characteristic absorption peak at 510 nm. The absorbance at 510 nm was measured, and the total flavonoid content was calculated using a rutin standard curve. The determination was performed following the instructions of a commercial plant biochemistry kit (AKPL015M, Boxbio Sci. & Tech. Co., Ltd., Beijing, China). For the determination of soluble protein content, fresh leaf samples (without drying) were used, and the content was analyzed with the Coomassie Brilliant Blue G-250 method [35], with results expressed on a fresh weight (FW) basis (mg g^{-1} FW). For each cultivar, four trees were selected as biological replicates. From each tree, four to five fully expanded leaves were collected and pooled to represent that tree. Three technical replicates were performed on each tree sample, and the average of the three technical replicates was used as one value for that tree. Thus, four biological replicates (four trees) were obtained for each cultivar.

2.7. Data Processing and Analysis

All data were analyzed using SPSS 25.0. To account for the nested structure of the experimental design (multiple cultivars within each ploidy level), nested ANOVA was used with ploidy as a fixed factor and cultivar as a random factor nested within ploidy. The significance of the ploidy effect was tested against the cultivar (ploidy) mean square. To assess the sensitivity of this design, a sensitivity analysis was performed in G*Power 3.1 for the ploidy effect given the nested design (four cultivars per ploidy level; total sample size = 8; numerator df = 1; number of groups = 2; denominator df = 6). The analysis indicated that, with $\alpha = 0.05$ and power = 0.80, the minimum detectable effect size was Cohen's f = 1.19. All data are presented as means ± SE, and $p < 0.05$ was considered statistically significant.

Pearson correlation analysis was performed to examine the relationships among leaf structural, photosynthetic, and metabolite traits. For each cultivar, all measured values of each trait were averaged to obtain a cultivar mean, and correlations were then calculated among the eight cultivar means. Significance was tested by a two-tailed test. Correlation analysis and heatmap visualization were performed using Origin 2025.

3. Results

3.1. Leaf Structural Traits

To investigate whether polyploidization alters leaf morphology and stomatal characteristics, we compared leaf structural traits between diploid and triploid cultivars.

3.1.1. Leaf Morphological Traits

The leaves of triploid cultivars were generally larger than those of diploids (Figure 2a–c). Leaf length ranged from 8.5 ± 0.3 cm (QY1) to 12.1 ± 0.4 cm (QY19), leaf width from 3.9 ± 0.1 cm (QY1) to 5.9 ± 0.2 cm (QY19), and leaf area from 21.8 ± 1.3 cm^2 (QY1) to 46.8 ± 2.6 cm^2 (QY19), with the triploid QY19 exhibiting the largest values for all three traits. Nested ANOVA revealed significant ploidy effects on leaf length ($p = 0.025$), leaf width ($p = 0.001$), and leaf area ($p = 0.002$), with the cultivar (ploidy) effects also being highly significant for all three traits ($p < 0.001$) (Table 1). In contrast, no statistically detectable ploidy effect was observed for leaf mass per area (LMA) ($p = 0.288$), whereas the cultivar (ploidy) effect was highly significant ($p < 0.001$), indicating that variation in LMA was associated mainly with genotypic differences among cultivars rather than with ploidy level (Table 1).

Table 1. Summary of nested ANOVA results for leaf structural, photosynthetic, and selected metabolite traits in diploid and triploid *C. axillaris*.

Trait Category	Trait	Ploidy Effect	Cultivar (Ploidy) Effect
Leaf structure	Leaf length (cm)	$F_{1,6} = 8.831$, $p = 0.025$	$F_{6,72} = 6.455$, $p < 0.001$
	Leaf width (cm)	$F_{1,6} = 35.208$, $p = 0.001$	$F_{6,72} = 4.729$, $p < 0.001$
	Leaf area (cm^2)	$F_{1,6} = 26.025$, $p = 0.002$	$F_{6,72} = 4.865$, $p < 0.001$
	LMA (g m^2)	$F_{1,6} = 1.361$, $p = 0.288$	$F_{6,72} = 6.031$, $p < 0.001$
	Stomatal density	$F_{1,6} = 43.503$, $p = 0.006$	$F_{6,16} = 1.301$, $p = 0.453$
	Stoma length (μm)	$F_{1,6} = 104.843$, $p < 0.001$	$F_{6,16} = 0.804$, $p = 0.575$
	Stoma width (μm)	$F_{1,6} = 8.107$, $p = 0.034$	$F_{6,16} = 3.094$, $p = 0.014$
Photosynthetic traits	P_n (μmol m^{-2} s^{-1})	$F_{1,6} = 0.966$, $p = 0.364$	$F_{6,32} = 139.006$, $p < 0.001$
	G_s (mmol m^{-2} s^{-1})	$F_{1,6} = 0.613$, $p = 0.463$	$F_{6,32} = 75.109$, $p < 0.001$
	T_r (mmol m^{-2} s^{-1})	$F_{1,6} = 0.461$, $p = 0.523$	$F_{6,32} = 38.723$, $p < 0.001$
	C_i (μmol mol^{-1})	$F_{1,6} = 4.054$, $p = 0.091$	$F_{6,32} = 2.195$, $p = 0.069$
	F_v/F_m	$F_{1,6} = 0.215$, $p = 0.660$	$F_{6,32} = 1.757$, $p = 0.140$

Table 1. *Cont.*

Trait Category	Trait	Ploidy Effect	Cultivar (Ploidy) Effect
Metabolites	Flavonoid content (mg g^{-1})	$F_{1,6} = 5.478$, $p = 0.058$	$F_{6,24} = 21.367$, $p < 0.001$
	Soluble protein content (mg g^{-1})	$F_{1,6} = 10.170$, $p = 0.019$	$F_{6,24} = 287.448$, $p < 0.001$
	Soluble sugar content (mg g^{-1})	$F_{1,6} = 2.700$, $p = 0.151$	$F_{6,24} = 21.766$, $p < 0.001$

Note: LMA, leaf mass per area; P_n, net photosynthetic rate; G_s, stomatal conductance; T_r, transpiration rate; C_i, intercellular CO_2 concentration; F_v/F_m, maximum photochemical efficiency of PSII. The ploidy effect compares diploid and triploid group means and was tested against the cultivar (ploidy) mean square. The cultivar (ploidy) effect compares variation among the four cultivars within each ploidy level. A significant ploidy effect indicates an overall difference between diploid and triploid groups, whereas a significant cultivar (ploidy) effect indicates that cultivars within a ploidy level differ from each other. $p < 0.05$ indicates statistical significance. Data were analyzed using nested ANOVA with ploidy as a fixed factor and cultivar as a random factor nested within ploidy.

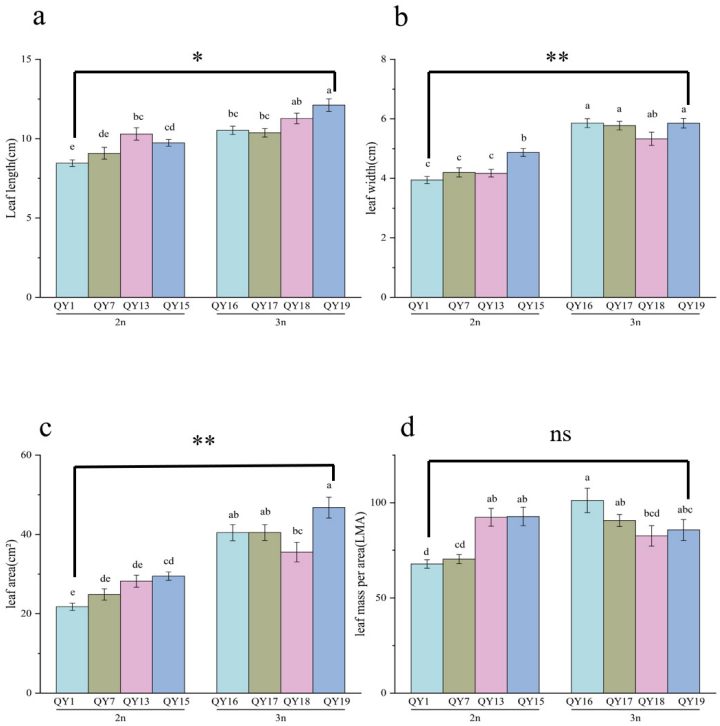


Figure 2. Leaf morphological characteristics of diploid and triploid *C. axillaris*. (**a**) Leaf length; (**b**) leaf width; (**c**) leaf area; (**d**) leaf mass per area (LMA). The bars show the mean ± SE ($n = 10$). Different lowercase letters indicate significant differences among the eight cultivars based on one-way ANOVA followed by Tukey's HSD test ($p < 0.05$). A horizontal line above the bars indicates the comparison between diploid and triploid groups based on the ploidy effect in nested ANOVA (* $p < 0.05$, ** $p < 0.01$, ns, not significant).

3.1.2. Stomatal Characteristics

Stomatal characteristics of diploid and triploid cultivars are shown in Figures 3 and 4. Stomatal density ranged from 200.84 ± 25.39 stomata mm^{-2} (QY16) to 412.07 ± 21.43 stomata mm^{-2} (QY1); stoma length ranged from 16.288 ± 0.609 µm (QY13) to 25.828 ± 1.341 µm (QY18); and stoma width ranged from 7.134 ± 0.633 µm (QY1) to 12.578 ± 0.466 µm (QY17). Nested ANOVA revealed significant ploidy effects on stomatal density ($p = 0.006$), stoma length ($p < 0.001$), and stoma width ($p = 0.034$). The cultivar (ploidy) effect was not significant for stomatal density ($p = 0.453$) or stoma length ($p = 0.575$) but was significant for stoma width ($p = 0.014$).

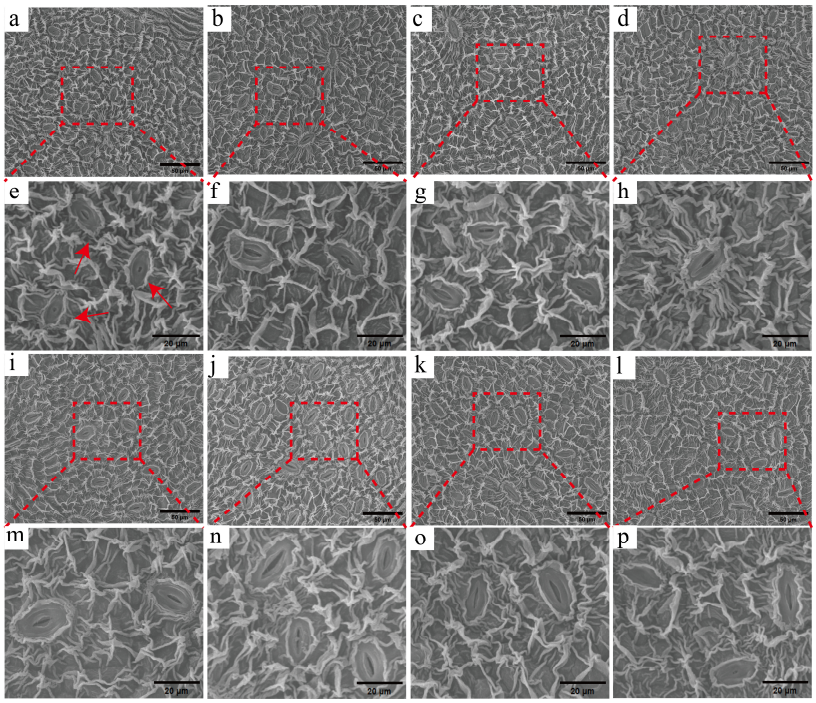


Figure 3. Leaf ultrastructure of diploid and triploid *C. axillaris*. Diploid: (**a**) QY1; (**b**) QY7; (**c**) QY13; (**d**) QY15. Triploid: (**i**) QY16; (**j**) QY17; (**k**) QY18; (**l**) QY19. (**e**) Enlarged view of the red dashed box in (**a**); (**f**) enlarged view of the red dashed box in (**b**); (**g**) enlarged view of the red dashed box in (**c**); (**h**) enlarged view of the red dashed box in (**d**); (**m**) enlarged view of the red dashed box in (**i**); (**n**) enlarged view of the red dashed box in (**j**); (**o**) enlarged view of the red dashed box in (**k**); (**p**) enlarged view of the red dashed box in (**l**). Red arrows indicate stomata.

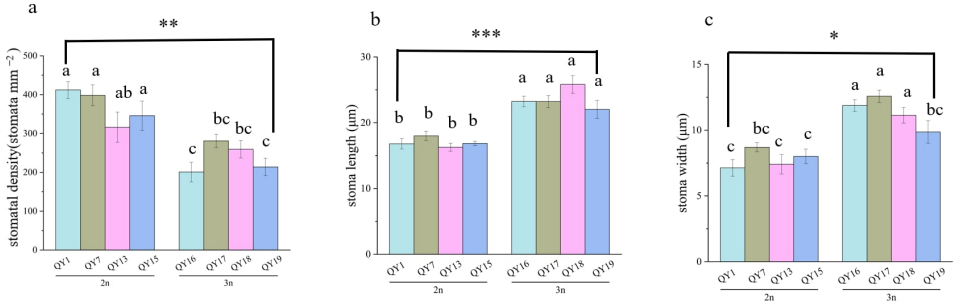


Figure 4. Stomatal characteristic differences in diploid and triploid *C. axillaris* leaves. (**a**) Stomatal density; (**b**) stoma length; (**c**) stoma width. The bars show the mean ± SE ($n = 3$). Different lowercase letters indicate significant differences among the eight cultivars based on one-way ANOVA followed by Tukey's HSD test ($p < 0.05$). A horizontal line above the bars indicates the comparison between diploid and triploid groups based on the ploidy effect in nested ANOVA (* $p < 0.05$, ** $p < 0.01$, *** $p < 0.001$; ns, not significant).

3.2. Photosynthetic Characteristics

3.2.1. Gas Exchange Parameters

P_n ranged from 3.091 ± 0.272 μmol m^{-2} s^{-1} (QY13) to 7.549 ± 0.359 μmol m^{-2} s^{-1} (QY16) among cultivars; G_s ranged from 43.833 ± 5.637 mmol m^{-2} s^{-1} (QY13) to 159.440 ± 12.071 mmol m^{-2} s^{-1} (QY16); T_r ranged from 2.089 ± 0.184 mmol m^{-2} s^{-1} (QY13) to 5.569 ± 0.297 mmol m^{-2} s^{-1} (QY16); and C_i ranged from 214.333 ± 36.950 μmol mol (QY16) to 295.667 ± 22.475 μmol mol (QY1) (Figure 5b–e). Nested ANOVA revealed that the ploidy effects on P_n ($p = 0.364$), G_s ($p = 0.463$), T_r ($p = 0.523$), and C_i ($p = 0.091$) were all non-significant. The cultivar (ploidy) effects were highly significant for P_n, G_s, and

T_r ($p < 0.001$), whereas the cultivar (ploidy) effect for C_i was not significant ($p = 0.069$) (Table 1). These results indicate that, except for C_i, variation in these gas exchange parameters may be associated mainly with genotypic differences among cultivars rather than with ploidy level.

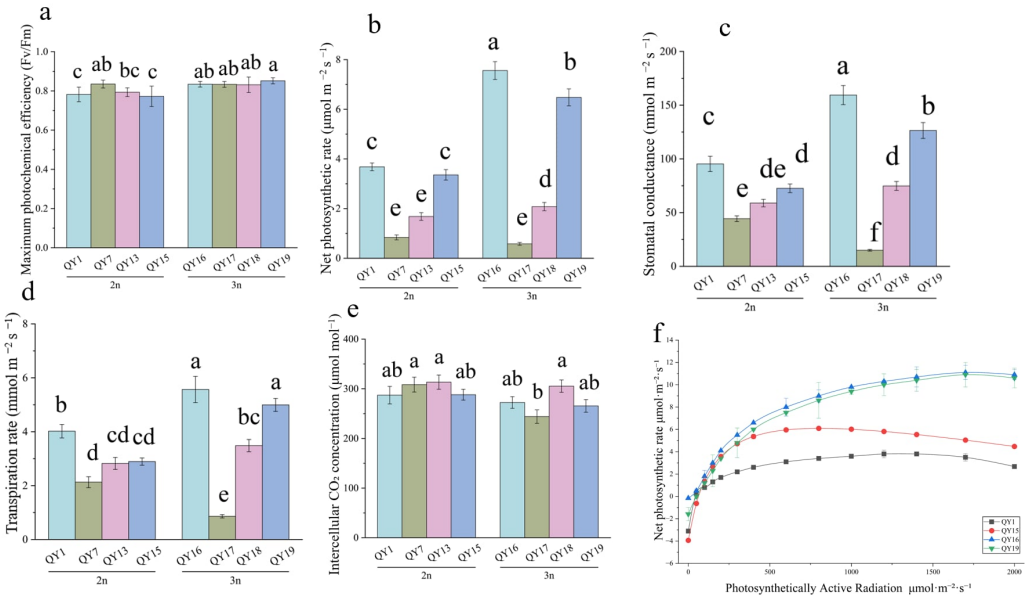


Figure 5. Chlorophyll fluorescence, photosynthetic parameters, and light-response curves of diploid and triploid *C. axillaris*. (**a**) Maximum photochemical efficiency (F_v/F_m); (**b**) net photosynthetic rate (P_n); (**c**) stomatal conductance (G_s); (**d**) transpiration rate (T_r); (**e**) intercellular CO_2 concentration (C_i); (**f**) photosynthetic light-response curves. Panels (**a**–**e**): bars show the mean ± SE ($n = 5$ biological replicates per cultivar). Panel (**f**): light-response curves measured on three biological replicates per cultivar ($n = 3$); data are means ± SE. Different lowercase letters indicate significant differences among the eight cultivars based on one-way ANOVA followed by Tukey's HSD test ($p < 0.05$). For panels (**a**–**e**), no statistically detectable ploidy effect was observed between the diploid and triploid groups based on nested ANOVA, and therefore no group-level comparison line is shown.

3.2.2. Chlorophyll Fluorescence Parameters

The maximum photochemical efficiency (F_v/F_m) ranged from 0.772 ± 0.051 (QY13) to 0.852 ± 0.015 (QY19) among cultivars, with all values falling within the normal range for healthy plants (Figure 5a). Nested ANOVA revealed that neither ploidy ($p = 0.660$) nor cultivar (ploidy) ($p = 0.140$) had a significant effect on F_v/F_m (Table 1), indicating that all tested cultivars maintained functionally intact photosystem II reaction centers under the experimental conditions.

3.2.3. Photosynthetic Light-Response Curves

To compare the photosynthetic response of diploid and triploid cultivars under different light intensities, light-response curves were measured for QY1, QY15, QY16, and QY19 (Figure 5f). Under low light intensities (0–600 μmol m^{-2} s^{-1}), P_n of all tested cultivars increased sharply with increasing PAR. As PAR continued to increase, the curves diverged: P_n of QY15 reached a plateau at around 800 μmol m^{-2} s^{-1}, whereas P_n of QY1, QY16, and QY19 continued to increase at higher irradiances. According to the fitted parameters (Table 2), the highest P_{max} and LSP were observed in QY16 (11.083 μmol m^{-2} s^{-1} and 1653 μmol m^{-2} s^{-1}, respectively), the lowest P_{max} in QY1 (4.021 μmol m^{-2} s^{-1}), and the lowest LSP in QY15 (817 μmol m^{-2} s^{-1}).

Table 2. Light-response curve parameters of four *C. axillaris* cultivars fitted with the modified rectangular hyperbola model.

Cultivar	Ploidy	Pmax (μmol m^{-2} s^{-1})	α (μmol μmol^{-1})	LSP (μmol m^{-2} s^{-1})
QY1	2x	4.021	0.0196	1316
QY15	2x	6.214	0.0248	817
QY16	3x	11.083	0.0301	1653
QY19	3x	10.852	0.0279	1624

Note: Pmax, maximum net photosynthetic rate; α, apparent quantum yield (AQY); LSP, light-saturation point. α was calculated from the low-light segment (0–200 μmol m^{-2} s^{-1}) of the light-response curves.

3.3. Leaf Metabolite Characteristics

To investigate the differences in flavonoid, soluble sugar, and soluble protein contents between ploidy levels, we measured the contents of these three metabolites in leaves. Flavonoid content ranged from 1.716 ± 0.143 mg g^{-1} (QY7) to 5.934 ± 0.495 mg g^{-1} (QY18) among cultivars; soluble protein content ranged from 2.259 ± 0.015 mg g^{-1} (QY1) to 9.498 ± 0.152 mg g^{-1} (QY18); and soluble sugar content ranged from 20.488 ± 0.544 mg g^{-1} (QY19) to 40.607 ± 1.327 mg g^{-1} (QY13) (Figure 6). Nested ANOVA revealed a significant ploidy effect on soluble protein content ($p = 0.019$), with the cultivar (ploidy) effect also being highly significant ($p < 0.001$) (Table 1), indicating that triploid cultivars as a group had higher soluble protein content, while genotypic differences among cultivars also contributed substantially to this trait. For flavonoid content, the ploidy effect was not significant ($p = 0.058$), whereas the cultivar (ploidy) effect was highly significant ($p < 0.001$). For soluble sugar content, the ploidy effect was not significant ($p = 0.151$), whereas the cultivar (ploidy) effect was highly significant ($p < 0.001$). Taken together, soluble protein was the only metabolite significantly and positively regulated by ploidy level, whereas flavonoid and soluble sugar accumulation were primarily driven by genotypic differences among cultivars.

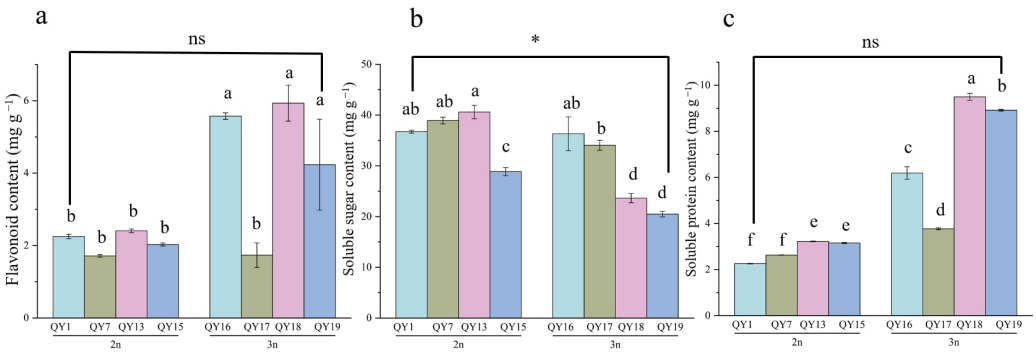


Figure 6. Metabolite differences in leaves of diploid and triploid *C. axillaris*. (**a**) Flavonoid content; (**b**) soluble sugar content; (**c**) soluble protein content. The bars show the mean ± SE ($n = 4$). Different lowercase letters indicate significant differences among the eight cultivars based on one-way ANOVA followed by Tukey's HSD test ($p < 0.05$). A horizontal line above the bars indicates the comparison between diploid and triploid groups based on the ploidy effect in nested ANOVA (* $p < 0.05$, ns, not significant).

3.4. Correlation Analysis Reveals Coordinated Trait Associations in C. axillaris

To explore the interrelationships among physiological, structural, and metabolic traits in diploid and triploid *C. axillaris*, an exploratory correlation analysis was performed on the cultivar means (Figure 7). Leaf area, leaf length, and leaf width were positively correlated with each other, consistent with their coordinated variation in leaf size. Stomatal density was negatively correlated with stoma length, stoma width, and leaf area, and positively

correlated with G_s. P_n was positively correlated with G_s and T_r, while no significant correlation was detected between P_n and C_i. Soluble protein content was positively correlated with leaf area, stoma length, flavonoid content, and P_n. F_v/F_m showed no significant correlation with the gas exchange parameters.

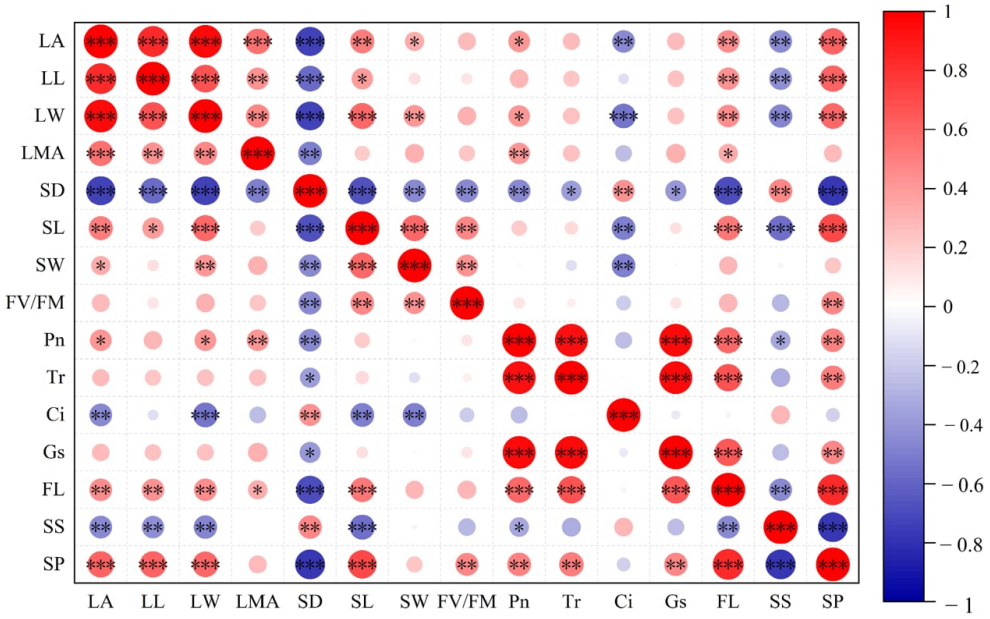


Figure 7. Correlation heatmap of leaf structural, photosynthetic, and metabolite traits in *C. axillaris*. Positive and negative correlations are shown in red and blue, respectively. Correlations were calculated using Pearson correlation coefficients based on cultivar means ($n = 8$). Asterisks indicate significant correlations (* $p < 0.05$, ** $p < 0.01$, *** $p < 0.001$). LA, leaf area; LL, leaf length; LW, leaf width; LMA, leaf mass per area; SD, stomatal density; SL, stoma length; SW, stoma width; F_v/F_m, maximum photochemical efficiency of PSII; P_n, net photosynthetic rate; T_r, transpiration rate; C_i, intercellular CO_2 concentration; G_s, stomatal conductance; FL, flavonoid content; SS, soluble sugar content; SP, soluble protein content.

4. Discussion

Natural polyploids are of considerable value in plant evolution and breeding; however, systematic studies on natural polyploids in *C. axillaris* remain scarce. In this study, diploid and natural triploid *C. axillaris* accessions were compared in terms of leaf structure, photosynthetic characteristics, and metabolite accumulation. Within the traits measured here, triploid accessions showed distinct leaf morphology and stomatal structure, along with higher soluble protein content, but these differences were not associated with a statistically detectable, general enhancement of net photosynthetic rate. Variation in photosynthetic parameters was mainly associated with cultivar (genotype) differences rather than with ploidy level per se.

4.1. Ploidy and Cultivar Effects on Leaf Structure

Polyploidy-induced organ gigantism is a common phenotypic effect in plants and has been reported in multiple species, including *Paulownia australis*, *Nicotiana tabacum*, *Betula platyphyllia*, and *Liriodendron* × *sinoamericanum* [27,36–38]. In the present study, the leaves of triploid *C. axillaris* cultivars were generally larger than those of diploids. Nested ANOVA revealed significant ploidy effects on leaf length ($p = 0.025$), leaf width ($p = 0.001$), and leaf area ($p = 0.002$), with the cultivar (ploidy) effects also being highly significant for all three traits ($p < 0.001$), indicating that these traits were affected by both ploidy and cultivar (genotype) differences. In contrast, no statistically detectable ploidy effect was observed

for leaf mass per area (LMA) ($p = 0.288$), and its variation was associated mainly with genotypic differences among cultivars (cultivar (ploidy) effect: $p < 0.001$).

Regarding stomatal characteristics, the responses to ploidy variation differ among species [39], but most studies indicate that polyploids generally exhibit larger stomata and lower stomatal density [40–43]. In this study, triploid cultivars showed significantly lower stomatal density and significantly greater stoma length and stoma width ($p = 0.006$, $p < 0.001$, and $p = 0.034$), consistent with previous reports. The cultivar (ploidy) effect was not significant for stomatal density ($p = 0.453$) or stoma length ($p = 0.575$), indicating that these two traits were mainly associated with ploidy and were relatively consistent among cultivars. However, the cultivar (ploidy) effect was significant for stoma width ($p = 0.014$), indicating that stoma width was affected not only by ploidy but also by cultivar (genotype) differences.

4.2. Ploidy and Cultivar Effects on Gas Exchange and Chlorophyll Fluorescence

Chlorophyll fluorescence is closely linked to several key processes of photosynthesis [44], and changes in its parameters can sensitively reflect the light energy conversion efficiency of photosystem II (PSII) reaction centers, the electron transport rate, and the plant's capacity to dissipate excess light energy as heat [45]. In the present study, the F_v/F_m values of different ploidy cultivars of C. axillaris ranged from 0.772 to 0.852, all within the normal range for healthy plants [46–48], indicating that the PSII reaction centers were functionally intact after dark adaptation, with no indication of photoinhibition at the time of measurement. Nested ANOVA showed that the ploidy effect on F_v/F_m was not significant ($p = 0.660$), nor was the cultivar (ploidy) effect ($p = 0.140$), indicating that F_v/F_m is a conservative physiological parameter that did not exhibit systematic differences between the tested diploid and triploid cultivars, with PSII photochemical efficiency maintained at normal levels in all cultivars.

Photosynthesis is the core metabolic process by which plants convert light energy into chemical energy, fix CO_2, and synthesize organic compounds [49]. Previous studies have shown that polyploidization can significantly enhance the photosynthetic capacity of some species, such as polyploid *Eucommia ulmoides* [50], *Ziziphus jujuba* [51], *Melissa officinalis* [52], and *Anoectochilus roxburghii* [53], all of which exhibit higher net photosynthetic rates than their diploid counterparts. However, in the present study, the ploidy effects on P_n, G_s, and T_r were all non-significant, whereas the cultivar (ploidy) effects were highly significant. This pattern suggests that variation in these three parameters may be associated mainly with genotypic differences among cultivars rather than with ploidy level per se. Neither the ploidy effect ($p = 0.091$) nor the cultivar (ploidy) effect ($p = 0.069$) on C_i was significant. Notably, although stomatal density, stoma length, and stoma width showed significant ploidy effects, no statistically detectable ploidy effects were observed for P_n, G_s, T_r, or C_i, indicating that the "larger but fewer" stomatal configuration did not translate into detectable differences in the gas exchange parameters measured here. This pattern is similar to that reported in polyploid *Populus* clones [23], in which net photosynthetic rate did not differ significantly among ploidy levels, whereas Pn varied by more than 37% among individual clones. Light-response curves were measured for only four representative cultivars (QY1, QY15, QY16, and QY19), with two cultivars per ploidy level. Although QY16 and QY19 maintained higher P_n at high PAR, this difference cannot be attributed to ploidy level because of the limited number of cultivars measured. It should therefore be regarded as a cultivar-specific characteristic rather than a general effect of triploidy. These results suggest that the effects of polyploidization on photosynthesis may be species-specific.

4.3. Ploidy and Cultivar Effects on Leaf Metabolite Accumulation

Polyploidization can systematically regulate plant metabolic networks and significantly influence the synthesis and accumulation of secondary metabolites [54]. In this study, the ploidy effect on soluble protein content was significant ($p = 0.019$), with triploid cultivars as a group exhibiting higher soluble protein content, consistent with observations in polyploid *Cannabis sativa* [55]. However, the higher soluble protein content in triploids did not correspond to a stronger photosynthetic capacity, suggesting that the increased proteins may not be photosynthesis-related proteins such as Rubisco. In *Morus alba* [56] and *Populus* [57], polyploid plants showed increased flavonoid metabolites, but in the present study no statistically detectable ploidy effect was observed for flavonoid content ($p = 0.058$), and its accumulation was associated mainly with genotypic differences among cultivars. The ploidy effect on soluble sugar content was not significant ($p = 0.151$). The cultivar (ploidy) effects on flavonoids, soluble proteins, and soluble sugars were all highly significant ($p < 0.001$), indicating that the accumulation of these three metabolites in leaves was strongly influenced by genotypic differences among cultivars.

4.4. Perspectives

The results of this study indicate that triploid *C. axillaris* accessions showed distinct leaf structure and higher soluble protein content, whereas variation in photosynthetic performance was mainly associated with cultivar (genotype) differences. Several limitations should also be noted. First, the correlation analysis was based on cultivar means ($n = 8$). Given this small sample size, the correlations in Figure 7 should be regarded as an exploratory analysis intended to illustrate general patterns rather than to establish definitive significance. Second, the ploidy effects observed here were based on four cultivars per ploidy level. A sensitivity analysis indicated that this design had 80% power to detect only effects of Cohen's f $\geq$ 1.19. Therefore, non-significant ploidy effects warrant cautious interpretation, as the design was underpowered to detect smaller effects. This sample size may therefore reduce the robustness of the ploidy-related conclusions, and further experiments with additional polyploid materials are planned to verify the present findings. Third, the genetic relatedness and independent origin of the triploid accessions have not yet been established, which should be considered when generalizing the observed ploidy effects.

Future studies could therefore measure chlorophyll a/b, starch, and Rubisco contents to clarify the relationship between soluble protein and photosynthetic performance, validate the ploidy effects with a larger number of cultivars, and evaluate fruit yield, fruit quality, stress resistance and other agronomic traits to clarify the role of triploid *C. axillaris* in breeding and production. In summary, these results provide data support for polyploid breeding and superior germplasm selection in *C. axillaris*.

5. Conclusions

This study provides the first systematic comparison of diploid and natural triploid *C. axillaris* in terms of leaf structure, photosynthetic characteristics, and selected metabolites. The main conclusions are as follows:

(1) Triploid cultivars generally had larger leaves than diploids, with lower stomatal density and greater stoma length and stoma width, i.e., a "larger but fewer" stomatal configuration. Nested ANOVA showed significant ploidy effects on stomatal density, stoma length, and stoma width. Among these traits, stomatal density and stoma length were mainly associated with ploidy, whereas stoma width was also significantly affected by cultivar (genotype) differences.

(2) Triploid cultivars showed significantly higher soluble protein content, no significant ploidy effect on flavonoid content, and no significant ploidy effect on soluble sugar content.

The accumulation of all three metabolite classes was strongly influenced by genotypic differences among cultivars.

(3) No statistically detectable ploidy effect was observed for net photosynthetic rate, stomatal conductance, or transpiration rate; variation in these parameters may be associated mainly with cultivar (genotype) differences rather than with a general advantage conferred by the triploid level. The F_v/F_m values of all cultivars were within the normal range for healthy plants.

In summary, among the traits measured here, the advantages of triploid *C. axillaris* were manifested in leaf structure and soluble protein content, whereas no statistically detectable, general enhancement of net photosynthetic rate was associated with the triploid level. These results provide data supporting polyploid breeding and superior germplasm selection in *C. axillaris*.

Supplementary Materials: The following supporting information can be downloaded at: https://www.mdpi.com/article/10.3390/biology15222120/s1, Table S1. Ploidy information of the eight *C. axillaris* accessions used in this study; Table S2. Germplasm sources and propagation information of the eight *C. axillaris* accessions used in this study;

Author Contributions: Conceptualization, T.Z., F.L. and Q.G.; methodology, T.Z., F.L., W.H., X.C., Y.L. and H.L.; software, T.Z., X.C. and Y.L.; validation, H.L., H.G., H.H., W.H. and J.L.; formal analysis, X.C. and Y.L.; investigation, F.L., W.H., H.L., H.G., H.H. and J.L.; resources, T.Z., F.L., Q.G., W.H., H.L., H.G., H.H. and J.L.; data curation, F.L., X.C., Y.L., H.G., H.H. and J.L.; writing—original draft preparation, T.Z. and F.L.; writing—review and editing, Q.G.; visualization, T.Z. and F.L.; supervision, Q.G.; funding acquisition, Q.G. All authors have read and agreed to the published version of the manuscript.

Funding: This research was funded by Project for Research, Development and Utilization of Germplasm Resources of *Choerospondias axillaris* (028010864), Talent Introduction Project Study of Nanjing Forestry University (GXL2018001) and Jiangsu Postgraduate Research and Practice Innovation Program Project (SJCX25_0424 and KYCX23_1250).

Institutional Review Board Statement: Not applicable.

Informed Consent Statement: Not applicable.

Data Availability Statement: All data generated or analyzed during this study are included in this article. All data are available from the first author upon request.

Acknowledgments: The authors gratefully acknowledge all lab members for their assistance in collecting *C. axillaris* leaves and data organization.

Conflicts of Interest: Authors Huashan Ling, Hequn Gu, Houlin He, and Jiyan Liu were employed by the company Jiangxi Qiyunshan Food Co., Ltd., Ganzhou 341300, China. The remaining authors declare that the research was conducted in the absence of any commercial or financial relationships that could be construed as a potential conflict of interest.

Abbreviations

The following abbreviations are used in this manuscript:

PAR	Photosynthetically active radiation
P_n	Net photosynthetic rate
G_s	Stomatal conductance
C_i	Intercellular CO_2 concentration
T_r	Transpiration rate
F_0	Initial fluorescence
F_m	Maximum fluorescence
F_v	Variable fluorescence

F_v/F_m	Maximum photochemical efficiency of PSII
PSII	Photosystem II
LMA	Leaf mass per area
DW	Dry weight
FW	Fresh weight
ANOVA	Analysis of variance
SE	Standard error

References

1. Mann, S.; Chakraborty, D.; Biswas, S. An Alternative Perspective of an Underutilized Fruit Tree *Choerospondias axillaris* in Health Promotion and Disease Prevention: A Review. *Food Biosci.* **2022**, *47*, 101609. [CrossRef]
2. Joshi, S.; Shrestha, L.K.; Kamachi, Y.; Malgras, V.; Pradhananga, M.A.; Pokhrel, B.P.; Nakato, T.; Pradhananga, R.R.; Ariga, K.; Yamauchi, Y. Synthesis and Characterizations of Nanoporous Carbon Derived from Lapsi (*Choerospondias axillaris*) Seed: Effect of Carbonization Conditions. *Adv. Powder Technol.* **2015**, *26*, 894–900. [CrossRef]
3. Li, Q.; Chen, J.; Li, T.; Liu, C.; Liu, W.; Liu, J. Comparison of Bioactivities and Phenolic Composition of *Choerospondias axillaris* Peels and Fleshes. *J. Sci. Food Agric.* **2016**, *96*, 2462–2471. [CrossRef] [PubMed]
4. Li, F.; Shen, Z.; Zhang, T.; Gao, X.; Ling, H.; Gu, H.; Liu, Z.; Liu, J.; Lin, C.; Guo, Q. First Insights into Ploidy and Genome Size Estimation in *Choerospondias axillaris* (Roxb.) B.L.Burtt & A.W.Hill (Anacardiaceae) Using Flow Cytometry and Genome Survey Sequencing. *Plants* **2025**, *14*, 3094. [CrossRef] [PubMed]
5. Neupane, S.; Bajracharya, S.; Thada, S.; Bakabal, A.; Khadka, R.B.; Devkota, H.P.; Pandey, J. Total Phenolic and Flavonoid Contents, and Preliminary Antioxidant, Xanthine Oxidase Inhibitory and Antibacterial Activities of Fruits of Lapsi (*Choerospondias axillaris* Roxb.), an Underutilized Wild Fruit of Nepal. *Appl. Sci.* **2023**, *13*, 8945. [CrossRef]
6. Wang, H.; Gao, X.D.; Zhou, G.C.; Cai, L.; Yao, W.B. In Vitro and in Vivo Antioxidant Activity of *Choerospondias axillaris* Aqueous Extract from Fruit. *Food Chem.* **2008**, *106*, 888–895. [CrossRef]
7. Rong, W.; Shi, Q.; Yang, Y.; Su, W.; Li, M.; Qin, M.; Bai, S.; Zhu, Q.; Wang, A. Fructus Choerospondiatis: A Comprehensive Review of Its Traditional Uses, Chemical Composition, Pharmacological Activities, and Clinical Studies. *J. Ethnopharmacol.* **2024**, *323*, 117696. [CrossRef] [PubMed]
8. Mann, S.; Sharma, A.; Sarkar, A.; Kharb, R.; Malhotra, R.; Datta, B.; Gupta, R.K.; Biswas, S. Evaluation of Anti-Inflammatory Effects of *Choerospondias axillaris* Fruit's Methanolic Extract in Synoviocytes and CIA Rat Model. *Curr. Pharm. Biotechnol.* **2020**, *21*, 596–604. [CrossRef] [PubMed]
9. Nguyen, D.D.; Nguyen, N.H.; Nguyen, T.T.; Phan, T.S.; Nguyen, V.D.; Grabe, M.; Johansson, R.; Lindgren, G.; Stjernstrom, N.E.; Soderberg, T.A. The Use of a Water Extract from the Bark of *Choerospondias axillaris* in the Treatment of Second Degree Burns. *Scand. J. Plast. Reconstr. Surg. Hand Surg.* **1996**, *30*, 139–144. [CrossRef] [PubMed]
10. Van de Peer, Y.; Mizrachi, E.; Marchal, K. The Evolutionary Significance of Polyploidy. *Nat. Rev. Genet.* **2017**, *18*, 411–424. [CrossRef] [PubMed]
11. Rothfels, C.J. Polyploid Phylogenetics. *New Phytol.* **2021**, *230*, 66–72. [CrossRef] [PubMed]
12. Zong, D.; Qiao, Z.; Zhou, J.; Li, P.; Gan, P.; Ren, M.; He, C. Chloroplast Genome Sequence of Triploid *Toxicodendron vernicifluum* and Comparative Analyses with Other Lacquer Chloroplast Genomes. *BMC Genom.* **2023**, *24*, 56. [CrossRef] [PubMed]
13. Zhang, X.; Feng, J.; Luo, Y.; Duan, X.; He, C.; Zong, D. In Vitro Propagation of Triploid *Toxicodendron vernicifluum* (Stokes) F. A. Barkl. *Vitr. Cell. Dev. Biol. Plant* **2024**, *60*, 783–791. [CrossRef]
14. Smarda, P.; Horova, L.; Knapek, O.; Dieck, H.; Dieck, M.; Razna, K.; Hrubik, P.; Orloci, L.; Papp, L.; Vesela, K.; et al. Multiple Haploids, Triploids, and Tetraploids Found in Modern-Day "Living Fossil" *Ginkgo biloba*. *Hortic. Res.* **2018**, *5*, 55. [CrossRef] [PubMed]
15. Huang, X.; Chen, J.; Yang, X.; Duan, S.; Long, C.; Ge, G.; Rong, J. Low Genetic Differentiation among Altitudes in Wild *Camellia oleifera*, a Subtropical Evergreen Hexaploid Plant. *Tree Genet. Genomes* **2018**, *14*, 21. [CrossRef]
16. Song, J.; Zhao, X.; Lin, B.; Zhang, S.; Lai, H.; Chen, F.; Huang, D.; Liu, J.; Hu, H.; Wang, J.; et al. Single Nucleotide Polymorphisms and Insertion/Deletion Variation Analysis of Octoploid and Decaploid Tropical Oil Tea *Camellia* populations Based on Whole-Genome Resequencing. *Plants* **2024**, *13*, 2955. [CrossRef] [PubMed]
17. Podwyszynska, M.; Markiewicz, M.; Broniarek-Niemiec, A.; Matysiak, B.; Marasek-Ciolakowska, A. Apple Autotetraploids with Enhanced Resistance to Apple Scab (*Venturia inaequalis*) Due to Genome Duplication-Phenotypic and Genetic Evaluation. *Int. J. Mol. Sci.* **2021**, *22*, 527. [CrossRef] [PubMed]
18. Lee, L. Citrus Polyploidy—Origins and Potential for Cultivar Improvement. *Aust. J. Agric. Res.* **1988**, *39*, 735–747. [CrossRef]
19. Matsuoka, Y. Evolution of Polyploid Triticum Wheats under Cultivation: The Role of Domestication, Natural Hybridization and Allopolyploid Speciation in Their Diversification. *Plant Cell Physiol.* **2011**, *52*, 750–764. [CrossRef] [PubMed]

20. Yan, H.; Han, J.; Jin, S.; Han, Z.; Si, Z.; Yan, S.; Xuan, L.; Yu, G.; Guan, X.; Fang, L.; et al. Post-Polyploidization Centromere Evolution in Cotton. *Nat. Genet.* **2025**, *57*, 1021–1030. [CrossRef] [PubMed]
21. Otto, S.P. The Evolutionary Consequences of Polyploidy. *Cell* **2007**, *131*, 452–462. [CrossRef] [PubMed]
22. Koziara-Ciupa, M.; Trojak-Goluch, A. The Effect of Polyploidisation on the Physiological Parameters, Biochemical Profile, and Tolerance to Abiotic and Biotic Stresses of Plants. *Agronomy* **2025**, *15*, 1918. [CrossRef]
23. Jiang, L.; Xu, X.; Cai, Q.; Han, R.; Tigabu, M.; Jiang, T.; Zhao, X. Variations in Growth and Photosynthetic Traits of Polyploid Poplar Hybrids and Clones in Northeast China. *Genes* **2022**, *13*, 2161. [CrossRef] [PubMed]
24. Zhao, X.; Li, Y.; Zheng, M.; Bian, X.; Liu, M.; Sun, Y.; Jiang, J.; Wang, F.; Li, S.; Cui, Y.; et al. Comparative Analysis of Growth and Photosynthetic Characteristics of (*Populus simonii* × *P. nigra*) × (*P. nigra* × *P. simonii*) Hybrid Clones of Different Ploidides. *PLoS ONE* **2015**, *10*, e0119259. [CrossRef] [PubMed]
25. Sun, Q.; Sun, H.; Li, L.; Bell, R.L. In Vitro Colchicine-Induced Polyploid Plantlet Production and Regeneration from Leaf Explants of the Diploid Pear (*Pyrus communis* L.) Cultivar, "Fertility.". *J. Hortic. Sci. Biotechnol.* **2009**, *84*, 548–552. [CrossRef]
26. Tan, F.-Q.; Tu, H.; Liang, W.-J.; Long, J.-M.; Wu, X.-M.; Zhang, H.-Y.; Guo, W.-W. Comparative Metabolic and Transcriptional Analysis of a Doubled Diploid and Its Diploid *Citrus* Rootstock (*C. junos* Cv. Ziyang Xiangcheng) Suggests Its Potential Value for Stress Resistance Improvement. *BMC Plant Biol.* **2015**, *15*, 89. [CrossRef] [PubMed]
27. Chen, T.; Sheng, Y.; Hao, Z.; Long, X.; Fu, F.; Liu, Y.; Tang, Z.; Ali, A.; Peng, Y.; Lu, L.; et al. Transcriptome and Proteome Analysis Suggest Enhanced Photosynthesis in Tetraploid *Liriodendron sino-americanum*. *Tree Physiol.* **2021**, *41*, 1953–1971. [CrossRef] [PubMed]
28. Xia, J.; Ma, Y.J.; Wang, Y.; Wang, J.W. Deciphering Transcriptome Profiles of Tetraploid *Artemisia annua* Plants with High Artemisinin Content. *Plant Physiol. Biochem.* **2018**, *130*, 112–126. [CrossRef] [PubMed]
29. Liu, Y.; Huang, X.; Gao, X.; Zhang, X.; Huang, H.; Li, W.; Zhang, Y. Tetraploidization Altered Phenotypic Traits and Metabolite Profile of Java Ginseng (*Talinum paniculatum* (Jacq.) Gaertn.). *Plants* **2025**, *14*, 480. [CrossRef] [PubMed]
30. Garnier, E.; Shipley, B.; Roumet, C.; Laurent, G. A Standardized Protocol for the Determination of Specific Leaf Area and Leaf Dry Matter Content. *Funct. Ecol.* **2001**, *15*, 688–695. [CrossRef]
31. Waite, M.; Sack, L. How Does Moss Photosynthesis Relate to Leaf and Canopy Structure? Trait Relationships for 10 Hawaiian Species of Contrasting Light Habitats. *New Phytol.* **2010**, *185*, 156–172. [CrossRef] [PubMed]
32. Li, F.; Hu, Y.; Jing, W.; Wang, Y.; Gao, X.; Guo, Q. Cytological, Physiological and Genotyping-by-Sequencing Analysis Revealing Dynamic Variation of Leaf Color in *Ginkgo biloba* L. *Horticulturae* **2025**, *11*, 395. [CrossRef]
33. Ye, Z.-P. A New Model for Relationship between Irradiance and the Rate of Photosynthesis in *Oryza sativa*. *Photosynthetica* **2007**, *45*, 637–640. [CrossRef]
34. DuBois, M.; Gilles, K.A.; Hamilton, J.K.; Rebers, P.A.; Smith, F. Colorimetric Method for Determination of Sugars and Related Substances. *Anal. Chem.* **1956**, *28*, 351–356. [CrossRef]
35. Bradford, M.M. A Rapid and Sensitive Method for the Quantitation of Microgram Quantities of Protein Utilizing the Principle of Protein-Dye Binding. *Anal. Biochem.* **1976**, *72*, 248–254. [CrossRef] [PubMed]
36. Wang, Z.; Fan, G.; Dong, Y.; Zhai, X.; Deng, M.; Zhao, Z.; Liu, W.; Cao, Y. Implications of Polyploidy Events on the Phenotype, Microstructure, and Proteome of *Paulownia australis*. *PLoS ONE* **2017**, *12*, e0172633. [CrossRef] [PubMed]
37. Landis, J.B.; Kurti, A.; Lawhorn, A.J.; Litt, A.; McCarthy, E.W. Differential Gene Expression with an Emphasis on Floral Organ Size Differences in Natural and Synthetic Polyploids of *Nicotiana tabacum* (Solanaceae). *Genes* **2020**, *11*, 1097. [CrossRef] [PubMed]
38. Mu, H.-Z.; Liu, Z.-J.; Lin, L.; Li, H.-Y.; Jiang, J.; Liu, G.-F. Transcriptomic Analysis of Phenotypic Changes in Birch (*Betula platyphylla*) Autotetraploids. *Int. J. Mol. Sci.* **2012**, *13*, 13012–13029. [CrossRef] [PubMed]
39. Martins Raizer, M.D.; Quisen, R.C.; Ferreira Valente, M.S.; Lopes, R.; Gomes Lopes, M.T. Morphological and Stomatal Characterization of *Heliconia chartacea* var. Sexy pink Induced Polyploidy. *Biosci. J.* **2019**, *35*, 222–235. [CrossRef]
40. Masterson, J. Stomatal Size in Fossil Plants: Evidence for Polyploidy in Majority of Angiosperms. *Science* **1994**, *264*, 421–424. [CrossRef] [PubMed]
41. Herawati, M.M.; Pudjihartati, E.; Pramono, S.; Sulistyaningsih, E.; Purwantoro, A. Obtaining *Artemisia cina* Polyploidy Through Plant Growth regulator Treatment in Shoot Culture. *AGRIVITA J. Agric. Sci.* **2015**, *37*, 178–184. [CrossRef]
42. Wang, J.; Wang, R.; Luo, F.; Du, W.; Hou, J.; Chen, G.; Tang, X.; Wu, J.; Wang, W.; Huang, B.; et al. Comparative Morphological, Physiological, and Transcriptomic Analyses of Diploid and Tetraploid Wucai (*Brassica campestris* L.). *Plants* **2024**, *13*, 2341. [CrossRef] [PubMed]
43. Cui, L.; Liu, Z.; Yin, Y.; Zou, Y.; Faizan, M.; Alam, P.; Yu, F. Research Progress of Chromosome Doubling and 2n Gametes of Ornamental Plants. *Horticulturae* **2023**, *9*, 752. [CrossRef]
44. Hikosaka, K. Photosynthesis, Chlorophyll Fluorescence and Photochemical Reflectance Index in Photoinhibited Leaves. *Funct. Plant Biol.* **2021**, *48*, 815–826. [CrossRef] [PubMed]
45. Yan, H.; Fu, K.; Li, J.; Li, M.; Li, S.; Dai, Z.; Jin, X. Photosynthesis, Chlorophyll Fluorescence, and Hormone Regulation in Tomato Exposed to Mechanical Wounding. *Plants* **2024**, *13*, 2594. [CrossRef] [PubMed]

46. Montoya, L.M.M.; Perez, A.A.A.; Giraldo Calderon, N.D.; Garces, L.A. Analysis of Cell Growth, Photosynthetic Behavior and the Fatty Acid Profile in *Tetraselmis subcordiformis* under Different Lighting Scenarios. *J. Appl. Phycol.* **2024**, *36*, 1679–1695. [CrossRef]
47. Canova, I.; Durkovic, J.; Hladka, D.; Lukacik, I. Changes in Stomatal Characteristics and Photochemical Efficiency during Leaf Development in Six Species of Sorbus. *Photosynthetica* **2012**, *50*, 635–640. [CrossRef]
48. Baker, N.R. Chlorophyll Fluorescence: A Probe of Photosynthesis in Vivo. *Annu. Rev. Plant Biol.* **2008**, *59*, 89–113. [CrossRef] [PubMed]
49. Croce, R.; Carmo-Silva, E.; Cho, Y.B.; Ermakova, M.; Harbinson, J.; Lawson, T.; McCormick, A.J.; Niyogi, K.K.; Ort, D.R.; Patel-Tupper, D.; et al. Perspectives on Improving Photosynthesis to Increase Crop Yield. *Plant Cell* **2024**, *36*, 3944–3973. [CrossRef] [PubMed]
50. Li, Y.; Yang, J.; Song, L.; Qi, Q.; Du, K.; Han, Q.; Kang, X. Study of Variation in the Growth, Photosynthesis, and Content of Secondary Metabolites in *Eucommia* Triploids. *Trees-Struct. Funct.* **2019**, *33*, 817–826. [CrossRef]
51. Liu, S.; Zhang, C.; Yang, W.; Li, X.; Hou, L.; Li, M.; Pang, X.; Li, Y. Hybrid Triploid Induced by Megaspore Chromosome Doubling in Jujube (*Ziziphus jujuba* Mill.) "maya" and Its Characteristics. *Forests* **2021**, *12*, 112. [CrossRef]
52. Bharati, R.; Gupta, A.; Novy, P.; Severova, L.; Sredl, K.; Ziarovska, J.; Fernandez-Cusimamani, E. Synthetic Polyploid Induction Influences Morphological, Physiological, and Photosynthetic Characteristics in *Melissa officinalis* L. *Front. Plant Sci.* **2023**, *14*, 1332428. [CrossRef] [PubMed]
53. Huang, X.; Ouyang, K.; Luo, Y.; Xie, G.; Yang, Y.; Zhang, J. A Comparative Study of Characteristics in Diploid and Tetraploid *Anoectochilus roxburghii*. *Front. Nutr.* **2022**, *9*, 1034751. [CrossRef] [PubMed]
54. Madani, H.; Escrich, A.; Hosseini, B.; Sanchez-Munoz, R.; Khojasteh, A.; Palazon, J. Effect of Polyploidy Induction on Natural Metabolite Production in Medicinal Plants. *Biomolecules* **2021**, *11*, 899. [CrossRef] [PubMed]
55. Bagheri, M.; Mansouri, H. Effect of Induced Polyploidy on Some Biochemical Parameters in *Cannabis sativa* L. *Appl. Biochem. Biotechnol.* **2015**, *175*, 2366–2375. [CrossRef] [PubMed]
56. Park, C.H.; Park, Y.E.; Yeo, H.J.; Yoon, J.S.; Park, S.-Y.; Kim, J.K.; Park, S.U. Comparative Analysis of Secondary Metabolites and Metabolic Profiling between Diploid and Tetraploid *Morus alba* L. *J. Agric. Food Chem.* **2021**, *69*, 1300–1307. [CrossRef] [PubMed]
57. Cheng, S.; Zong, Y.; Wang, X. Sub-Genome Polyploidization Effects on Metabolomic Signatures in Triploid Hybrids of *Populus*. *Forests* **2019**, *10*, 1091. [CrossRef]

Disclaimer/Publisher's Note: The statements, opinions and data contained in all publications are solely those of the individual author(s) and contributor(s) and not of MDPI and/or the editor(s). MDPI and/or the editor(s) disclaim responsibility for any injury to people or property resulting from any ideas, methods, instructions or products referred to in the content.